



**AFRL-RX-WP-TP-2011-4361**

**AN ULTRASONIC GUIDED WAVE METHOD TO  
ESTIMATE APPLIED BIAXIAL LOADS (PREPRINT)**

**Fan, Shi, Jennifer E. Michaels, and Sang Jun Lee**

**Georgia Tech Research Group**

**NOVEMBER 2011**

**Approved for public release; distribution unlimited.**

*See additional restrictions described on inside pages*

**STINFO COPY**

**AIR FORCE RESEARCH LABORATORY  
MATERIALS AND MANUFACTURING DIRECTORATE  
WRIGHT-PATTERSON AIR FORCE BASE, OH 45433-7750  
AIR FORCE MATERIEL COMMAND  
UNITED STATES AIR FORCE**

<b>REPORT DOCUMENTATION PAGE</b>				<i>Form Approved</i> OMB No. 0704-0188	
<p>The public reporting burden for this collection of information is estimated to average 1 hour per response, including the time for reviewing instructions, searching existing data sources, gathering and maintaining the data needed, and completing and reviewing the collection of information. Send comments regarding this burden estimate or any other aspect of this collection of information, including suggestions for reducing this burden, to Department of Defense, Washington Headquarters Services, Directorate for Information Operations and Reports (0704-0188), 1215 Jefferson Davis Highway, Suite 1204, Arlington, VA 22202-4302. Respondents should be aware that notwithstanding any other provision of law, no person shall be subject to any penalty for failing to comply with a collection of information if it does not display a currently valid OMB control number. <b>PLEASE DO NOT RETURN YOUR FORM TO THE ABOVE ADDRESS.</b></p>					
<b>1. REPORT DATE (DD-MM-YY)</b> November 2011		<b>2. REPORT TYPE</b> Technical Paper		<b>3. DATES COVERED (From - To)</b> 1 November 2011 – 1 November 2011	
<b>4. TITLE AND SUBTITLE</b> AN ULTRASONIC GUIDED WAVE METHOD TO ESTIMATE APPLIED BIAXIAL LOADS (PREPRINT)				<b>5a. CONTRACT NUMBER</b> FA8650-09-C-5206	
				<b>5b. GRANT NUMBER</b>	
				<b>5c. PROGRAM ELEMENT NUMBER</b> 62102F	
<b>6. AUTHOR(S)</b> Fan Shi, Jennifer E. Michaels, and Sang Jun Lee				<b>5d. PROJECT NUMBER</b> 4349	
				<b>5e. TASK NUMBER</b> 41	
				<b>5f. WORK UNIT NUMBER</b> LP106300	
<b>7. PERFORMING ORGANIZATION NAME(S) AND ADDRESS(ES)</b>  Georgia Tech Research Group 305 10th Street NW Atlanta, GA 30332				<b>8. PERFORMING ORGANIZATION REPORT NUMBER</b>	
<b>9. SPONSORING/MONITORING AGENCY NAME(S) AND ADDRESS(ES)</b>  Air Force Research Laboratory Materials and Manufacturing Directorate Wright-Patterson Air Force Base, OH 45433-7750 Air Force Materiel Command United States Air Force				<b>10. SPONSORING/MONITORING AGENCY ACRONYM(S)</b>  AFRL/RXLP	
				<b>11. SPONSORING/MONITORING AGENCY REPORT NUMBER(S)</b> AFRL-RX-WP-TP-2011-4361	
<b>12. DISTRIBUTION/AVAILABILITY STATEMENT</b> Approved for public release; distribution unlimited.					
<b>13. SUPPLEMENTARY NOTES</b> This work was funded in whole or in part by Department of the Air Force contract FA8650-09-C-5206. The U.S. Government has for itself and others acting on its behalf an unlimited, paid-up, nonexclusive, irrevocable worldwide license to use, modify, reproduce, release, perform, display, or disclose the work by or on behalf of the U.S. Government. PA Case Number and clearance date: 88ABW-2011-4593, 23Aug 2011. Preprint journal article to be submitted to Review of Progress in Quantitative NDE. This document contains color.					
<b>14. ABSTRACT</b> This paper will describe the development of a protocol for probabilistic reliability assessment for SHM systems as well as present an experimental demonstration for a vibration-based structural damage sensing system. The results of the full validation study highlight the general protocol feasibility, emphasize the importance of evaluating key application characteristics prior to the POD study, and demonstrate an approach to quantify varying sensor durability on the POD performance. Challenges remain to properly address long time-scale effects with accelerated testing and large testing requirements due to the independence of the inspection of each flaw location.					
<b>15. SUBJECT TERMS</b> model-assisted POD evaluation, probability of detection (POD), reliability, structural health monitoring					
<b>16. SECURITY CLASSIFICATION OF:</b>			<b>17. LIMITATION OF ABSTRACT:</b> SAR	<b>18. NUMBER OF PAGES</b> 16	<b>19a. NAME OF RESPONSIBLE PERSON (Monitor)</b> Charlie Buynak <b>19b. TELEPHONE NUMBER (Include Area Code)</b> N/A
<b>a. REPORT</b> Unclassified	<b>b. ABSTRACT</b> Unclassified	<b>c. THIS PAGE</b> Unclassified			

# AN ULTRASONIC GUIDED WAVE METHOD TO ESTIMATE APPLIED BIAXIAL LOADS

Fan Shi, Jennifer E. Michaels, and Sang Jun Lee

School of Electrical and Computer Engineering,  
Georgia Institute of Technology, Atlanta, Georgia 30332-0250

**ABSTRACT.** Guided wave propagation in a homogeneous plate is known to be sensitive to both temperature changes and applied stress variations. Here we consider the inverse problem of recovering biaxial stresses from measured changes in phase velocity at multiple propagation directions using a single mode at a specific frequency. These changes depend upon both the magnitude and orientation of the principle stresses. Although there is no closed form solution, prior results indicate that phase velocity changes exhibit a sinusoidal angular dependence. Here it is shown that all sinusoidal coefficients can be estimated from a single uniaxial loading experiment. The general biaxial inverse problem can thus be solved by fitting an appropriate sinusoid to measured phase velocity versus propagation angle, and relating the coefficients to the unknown stresses. The phase velocity data are obtained from direct arrivals between guided wave transducers whose direct paths of propagation are oriented at different angles. This method is applied to experimental sparse array data recorded during a fatigue test, and the additional complication of the resulting fatigue cracks interfering with some of the direct arrivals is addressed via proper selection of transducer pairs. Results show that applied stresses can be successfully recovered from the measured changes in guided wave signals.

**Key words:** Acoustoelasticity, Lamb waves, Load estimation

**PACS:** 43.20.Bi, 43.35.Cg, 46.40.Cd

## INTRODUCTION

Guided waves such as Lamb waves play a significant role in nondestructive evaluation (NDE) and structural health monitoring (SHM) techniques, which generally require or assume insensitivity to varying environmental and operational conditions. However, guided ultrasonic waves are well-known to have unavoidable sensitivity to environmental changes such as temperature, surface wetting and applied loads. However, applied loads can also open tightly closed fatigue cracks, so it is of interest to know the current loading state. This paper describes an inverse method to estimate the stress tensor as a homogeneous biaxial load is applied, which is based on the forward problem of calculating dispersion curves for acoustoelastic Lamb waves [1]. The principal stress components and orientation are estimated from a sinusoidal fit of ultrasonic data collected from the same spatially distributed array that is being used to detect and characterize damage. The proposed method is experimentally validated using fatigue test data acquired on an aluminum plate from an array of spatially distributed piezoelectric. To minimize scattering effects caused by growing fatigue cracks, a subset of all available transducer pairs is selected and used to obtain a better sinusoid fit.

## BACKGROUND

Consider a homogenous, isotropic aluminum plate with thickness  $d$  and infinite in extent as shown in Figure 1. Biaxial stresses  $\sigma_{11}$  and  $\sigma_{22}$  are applied along the  $x_1$  and  $x_2$  axes of a rectilinear coordinate system  $x_i = (x_1, x_2, x_3)$ , which are rotated by an angle  $\alpha$  from a measurement coordinate system indicated by  $(x_1', x_2', x_3')$ . Assume that ultrasonic guided waves are propagating along a direction that makes an angle  $\theta$  with respect to the  $x_1$  axis and  $\theta'$  with respect to the  $x_1'$  axis.

As per previous work, the theory for acoustoelastic Lamb wave propagation has been developed [1] for biaxial loads and an arbitrary direction of propagation. Results show that isotropic dispersion curves for a stress-free plate become anisotropic with phase velocities becoming angle and stress dependent for a specified mode and frequency. Changes of phase velocity with load can be accurately approximated as a sinusoidal function with respect to the propagation angles as shown in Figure 2 for the fundamental symmetric ( $S_0$ ) mode.

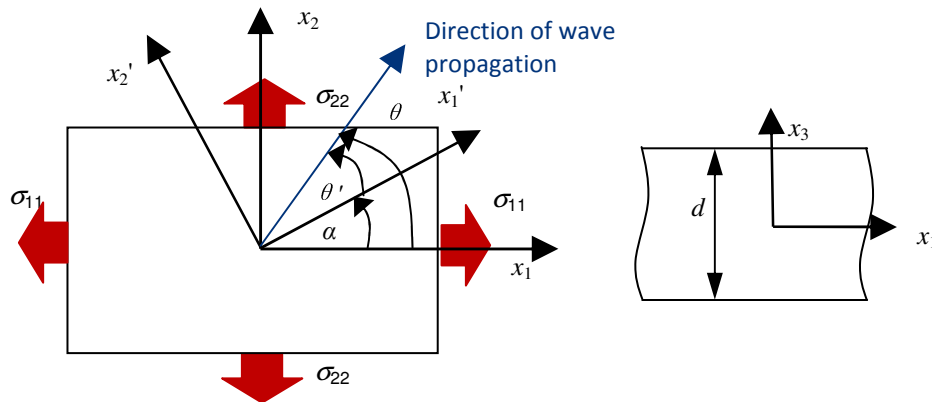


**FIGURE 1.** Geometry for Lamb wave propagation under applied biaxial stresses.

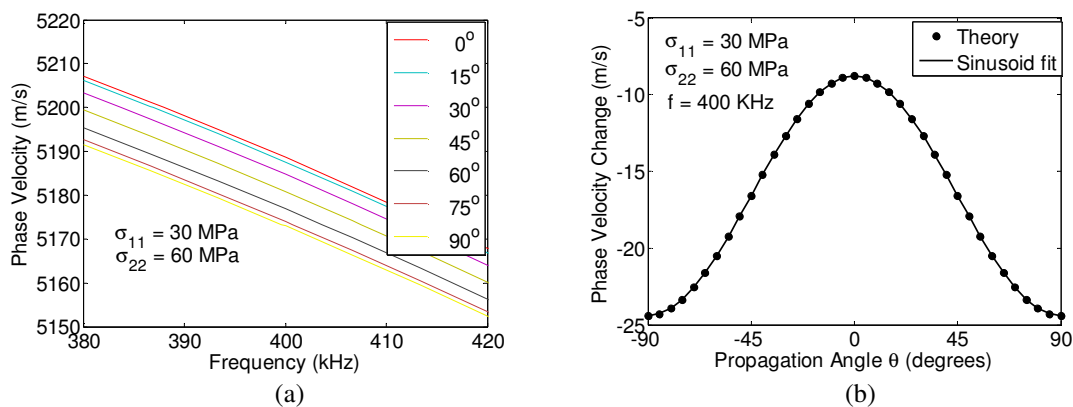


**FIGURE 2.** (a) Dispersion curves for the  $S_0$  mode when  $\sigma_{11} = 30$  MPa,  $\sigma_{22} = 60$  MPa for different propagation angles. (b) Changes of phase velocity for the  $S_0$  mode when  $\sigma_{11} = 30$  MPa,  $\sigma_{22} = 60$  MPa at 400 kHz as a function of propagation angle.

## LOAD ESTIMATION PROCEDURE

Based on the theory for acoustoelastic guided wave under a uniaxial load, the phase velocity change  $\Delta c_p$  for a given frequency and Lamb mode has the following form [2]:

$$\Delta c_p \Big|_{\sigma_{22}=0} = \sigma_{11}(K_1 \cos^2 \theta + K_2 \sin^2 \theta) \quad (1)$$

$$\Delta c_p \Big|_{\sigma_{11}=0} = \sigma_{22}(K_3 \cos^2 \theta + K_4 \sin^2 \theta) \quad (2)$$

In these equations  $\sigma_{11}$  and  $\sigma_{22}$  are uniaxial applied stresses in the  $x_1$  and  $x_2$  directions, respectively,  $\theta$  is the direction of Lamb wave propagation in the principal (unprimed) coordinate system, and  $K_1$ ,  $K_2$ ,  $K_3$  and  $K_4$  are the four acoustoelastic constants for the particular frequency, mode and loading direction. These equations are the same form as for non-dispersive bulk and Rayleigh waves, although the acoustoelastic constants for Lamb waves are frequency and mode-dependent even for homogeneous and isotropic media [3].

A combined equation for an arbitrary biaxial load can be deduced by first noting that the four acoustoelastic constants can be reduced to two (i.e.,  $K_1 = K_4$ ,  $K_2 = K_3$ ) because of symmetry. Next, we assume a combined sinusoidal function to describe the changes of phase velocity as a linear combination of the two uniaxial loading cases, which can be expressed as follows:

$$\Delta c_p(\theta) = (K_1\sigma_{11} + K_2\sigma_{22})\cos^2 \theta + (K_2\sigma_{11} + K_1\sigma_{22})\sin^2 \theta. \quad (3)$$

As written above, changes in phase velocity are expressed in the principal axis system, which may not coincide with the measurement system, which is rotated by  $\alpha$  from the principal axis system. After some algebra, Eq. (3) can be rewritten as follows:

$$\begin{aligned} \Delta c_p(\theta') &= (K_1\sigma_{11} + K_2\sigma_{22})\cos^2(\theta' + \alpha) + (K_2\sigma_{11} + K_1\sigma_{22})\sin^2(\theta' + \alpha) \\ &= a_0 + a_1 \cos(2\theta') + a_2 \sin(2\theta'). \end{aligned} \quad (4)$$

In this equation,

$$\begin{aligned} a_0 &= \frac{1}{2}(K_1 + K_2)(\sigma_{11} + \sigma_{22}), \quad a_1 = \frac{1}{2}(K_1 - K_2)(\sigma_{11} - \sigma_{22})\cos(2\alpha), \quad \text{and} \\ a_2 &= -\frac{1}{2}(K_1 - K_2)(\sigma_{11} - \sigma_{22})\sin(2\alpha) \end{aligned} \quad (5)$$

Numerical simulations were performed to validate Eq. (4). First, phase velocity changes for the  $S_0$  mode at 400 kHz were simulated for multiple uniaxial stress conditions for  $\sigma_{11} = 0$  and  $\sigma_{22}$  varying from 0 MPa to 100 MPa in steps of 10 MPa; the propagation angle  $\theta$  varied from 0 degree to 90 degrees in steps of 5 degrees. Second,  $K_1$  and  $K_2$  were estimated by least-squares using Eq. (2) for the multiple known uniaxial cases; their values were consistent for all cases considered. Third, theoretical phase velocity changes were calculated as a function of propagation angle for multiple cases of  $\alpha$ ,  $\sigma_{11}$  and  $\sigma_{22}$  as described in [1]. Finally, constants  $K_1$  and  $K_2$  determined from the first step were used in Eq. (4) to estimate the changes of phase velocity for the multiple cases of  $\alpha$ ,  $\sigma_{11}$  and  $\sigma_{22}$ . The results of Eq. (4) were then compared to calculated curves and were found to be in excellent agreement for all cases. Typical results are shown in Figure 3 for  $\alpha = 30$  degrees,  $\sigma_{11} = 30$  MPa and  $\sigma_{22} = 60$  MPa. Therefore, the assumed sinusoidal dependence and linear combination of uniaxial loading cases for biaxial loading is numerically confirmed.

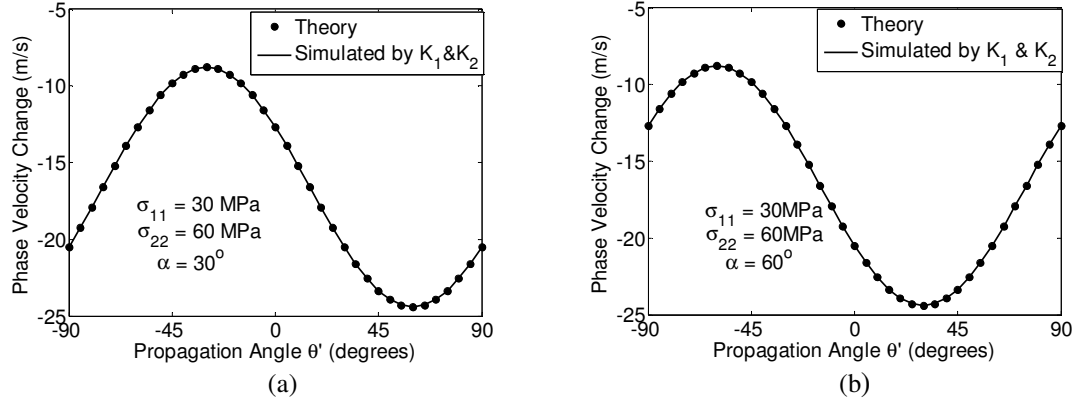


**FIGURE 3.** Phase velocity changes for the  $S_0$  mode at 400 kHz versus propagation angle. (a)  $\sigma_{11} = 30$  MPa,  $\sigma_{22} = 60$  MPa, and  $\alpha = 30$  degrees. (b)  $\sigma_{11} = 30$  MPa,  $\sigma_{22} = 60$  MPa, and  $\alpha = 60$  degrees.

The approach to the inverse problem can be readily seen by considering Eq. (4), which described the expected sinusoidal form of the  $\Delta c_p$  vs.  $\theta'$  data. Once  $K_1$  and  $K_2$  are obtained, the constants  $a_0$ ,  $a_1$  and  $a_2$  can be determined via least-squares. Finally, the unknown biaxial loads  $\sigma_{11}$  and  $\sigma_{22}$  along with the orientation angle  $\alpha$  can be expressed in terms of  $a_0$ ,  $a_1$  and  $a_2$  as follows:

$$\sigma_{11} = \frac{a_0 \cos(2\alpha)(K_1 - K_2) + a_1(K_1 + K_2)}{\cos(2\alpha)(K_1^2 - K_2^2)}, \quad \sigma_{22} = \frac{a_0 \cos(2\alpha)(K_2 - K_1) + a_1(K_1 + K_2)}{\cos(2\alpha)(K_2^2 - K_1^2)}, \quad (5)$$

and  $\alpha = \frac{1}{2} \arctan\left(-\frac{a_2}{a_1}\right)$ .

This procedure is used in the subsequent sections to estimate stresses from measurements of phase velocity changes with load.

## EXPERIMENTAL VALIDATION

A fatigue test was performed with an array of six surface-bonded PZT transducers on a 6061 aluminum plate as shown in Figure 4. The specimen was fatigued using a sinusoidal tension-tension profile from 16.5 MPa to 165 MPa at 3 Hz. Ultrasonic signals from the 15 unique transducer pairs were recorded for uniaxial loads ranging from 0 to 115 MPa in steps of 11.5 MPa for each data set. A total of fourteen data sets were recorded, where each data set contains 11 static loading measurements. Additional information, including the growth of fatigue cracks, is summarized in [4].

Guided waves were generated by a broadband chirp excitation. Then, the measured signals were filtered using a 7 cycle, Hanning windowed, 400 kHz tone burst signal [5]. In this paper, the  $S_0$  Lamb wave mode was chosen for analysis because it has clear first arrivals from all the transducer pairs, which is more convenient than the slower  $A_0$  mode for accurately extracting phase velocity changes.

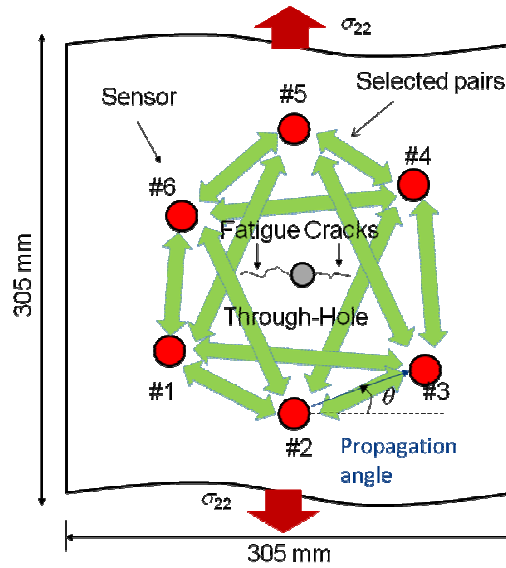


FIGURE 4. Drawing of the specimen and transducer geometry (not to scale).

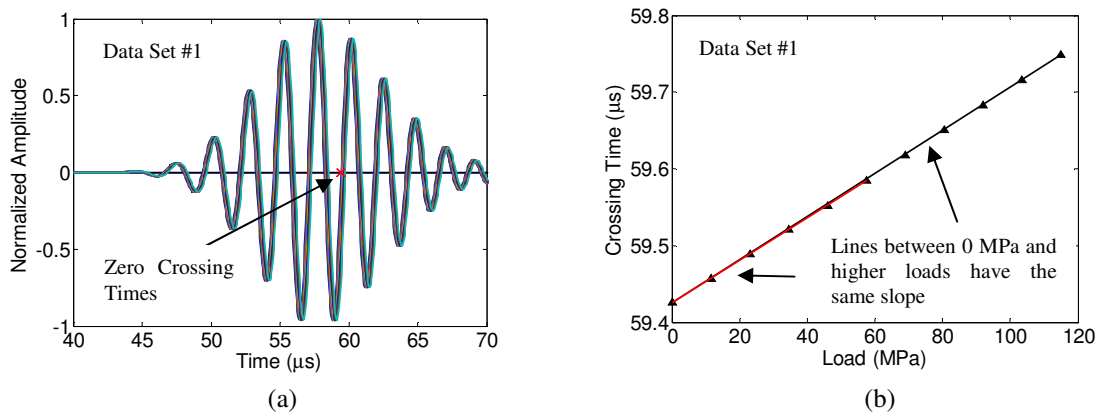
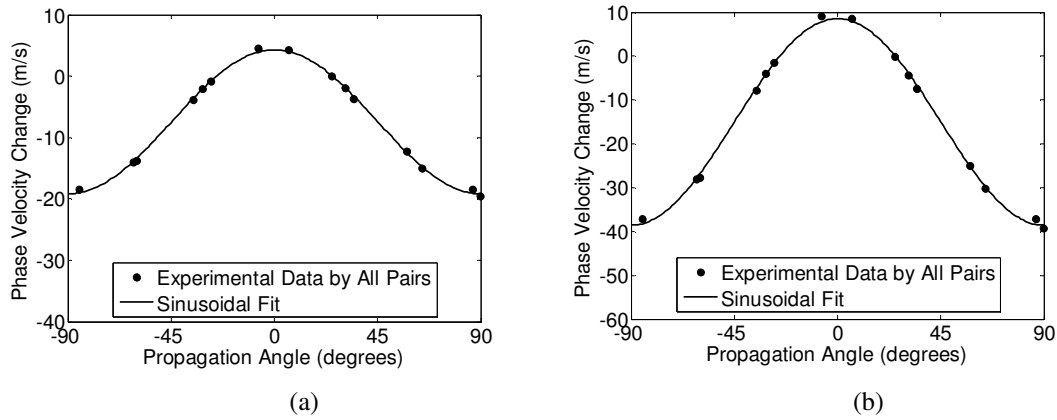


FIGURE 5. (a) First arrivals of transducer pair #2–5, data set #1, for the 11 uniaxial loading conditions (baseline, no crack). (b) Zero crossing times with respect to loads for transducer pair #2–5, data set #1.

Changes in received signals from each transducer pair caused by uniaxial loading were first investigated by examining zero crossing times within the first arrival of each signal. For example, Figure 5(a) shows received signals from transducer pair #2–5 and data set #1 (no cracks) for the 11 uniaxial loads. Small time shifts of the first arrival with each load increment can be seen, and a linear relationship between zero crossing time and applied load is observed as shown in Figure 5(b). Changes in phase velocity for the 11 loading conditions and 15 transducer pairs, which refer to different propagation angles, were extracted from first arrivals and zero crossing times. Constants  $K_1$  and  $K_2$  were estimated from all transducer pairs and known loading conditions of data set #1 via Eq. (2).

Loading conditions were assumed to be unknown for all other data sets. Constants  $a_0$ ,  $a_1$ , and  $a_2$  were estimated via a sinusoidal least squares fit of phase velocity changes vs. propagation angle using Eq. (4), and  $\sigma_{11}$ ,  $\sigma_{22}$  and  $\alpha$  were calculated from  $a_0$ ,  $a_1$ , and  $a_2$  using Eq. (5). As an example, Figure 6 shows the sinusoidal fit for changes in phase velocity with respect to the propagation angle using all the transducer pairs of data set #2 for two different loading conditions. Table 1 shows that the recovered loads and orientation angle are in good agreement with actual values.



**FIGURE 6.** Example experimental data and sinusoidal fit for data set #2. (a)  $\sigma_{11} = 0$  MPa,  $\sigma_{22} = 57.5$  MPa. (b)  $\sigma_{11} = 0$  MPa,  $\sigma_{22} = 115$  MPa.

**TABLE 1.** Estimated stresses and angle for two loads from data set #2

	$\sigma_{11}$ (MPa)	$\sigma_{22}$ (MPa)	$\alpha$ (degree)	$\sigma_{11}$ (MPa)	$\sigma_{22}$ (MPa)	$\alpha$ (degree)
Actual	0	57.5	0	0	115	0
Estimated	-1.24	55.65	-0.15	-2.20	112.07	-0.03

However, as cracks appear and grow in the later data sets, the ultrasonic signals obtained from the transducer pairs whose direct paths travel through cracks become much more complicated. As an example, Figure 7(a) shows both nonlinear time shifts of the first arrivals and significant amplitude decreases from data set #10 (two cracks) because the fatigue cracks interfered with the direct ultrasonic arrivals. Figure 7(b) shows that when the two cracks open, the zero crossing times are no longer linear with respect to the applied load, which will clearly affect the accuracy of the computed changes in phase velocity with load.

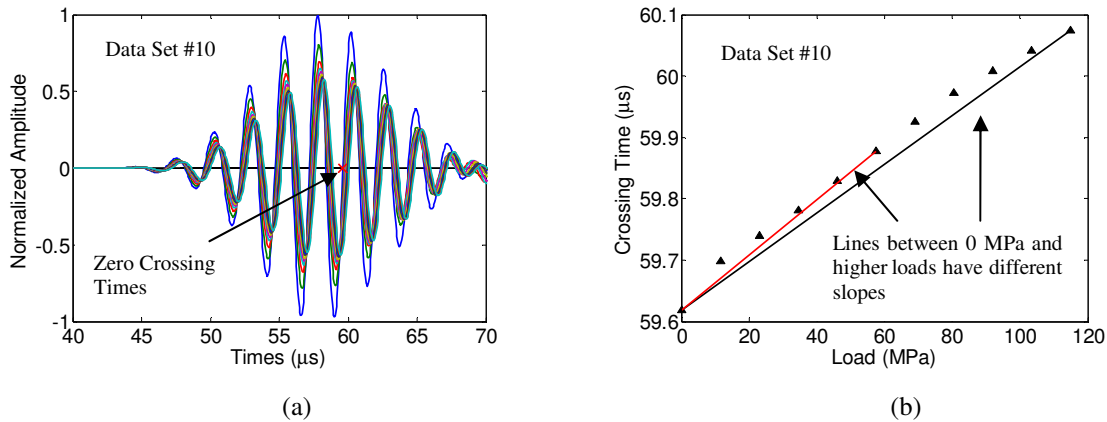


**FIGURE 7.** (a) First arrivals of 11 uniaxial loading conditions for transducer pair #2–5, data set #10 (two cracks). (b) Zero crossing times with respect to loads for pair #2–5, data set #14.



The complication of cracks interfering with the direct arrivals is mitigated by excluding some of the signals from the sinusoidal fit. Referring to Figure 4, it can be seen that the direct arrivals of three transducer pairs travel directly through the cracked region: #1-4, #2-5 and #3-6. If these pairs are excluded, the effects of cracks are minimized. Figure 8 shows the sinusoidal fit for changes in phase velocity with respect to the propagation angle from two loading conditions using both the 12 selected pairs and all 15 pairs.

Finally,  $\sigma_{11}$  and  $\sigma_{22}$  along with the angle  $\alpha$  were calculated from  $a_0$ ,  $a_1$ , and  $a_2$  from Eq. (5). Figure 9(a) shows the estimated uniaxial loads and angle when actual  $\sigma_{11} = 0$  MPa and  $\sigma_{22} = 57.5$  MPa, and Figure 9(b) shows the results for  $\sigma_{11} = 0$  MPa and  $\sigma_{22} = 115$  MPa. Results for both the selected pairs and all the pairs are shown for comparison, where it can be seen that excluding some of the transducer pairs considerably improved results for the later data sets.

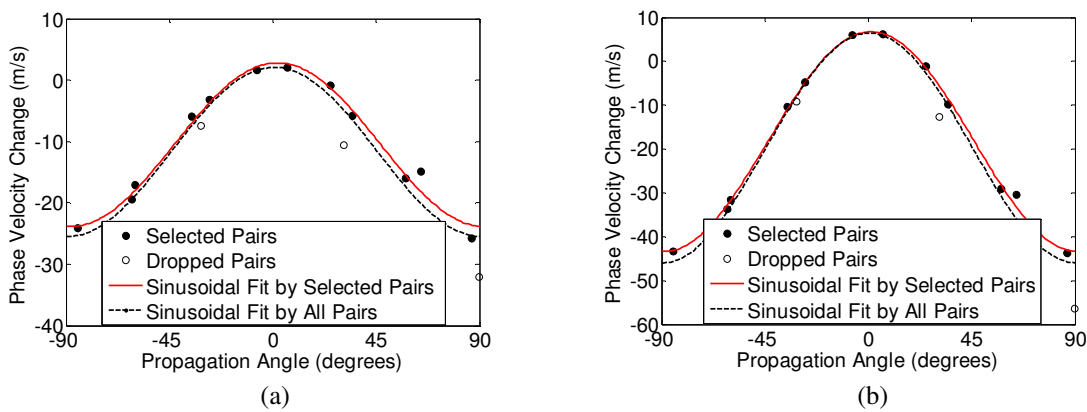


**FIGURE 8.** Experimental data and sinusoidal fit of phase velocity changes for data set #10. (a)  $\sigma_{11} = 0$  MPa,  $\sigma_{22} = 57.5$  MPa, (b)  $\sigma_{11} = 0$  MPa,  $\sigma_{22} = 115$  MPa.

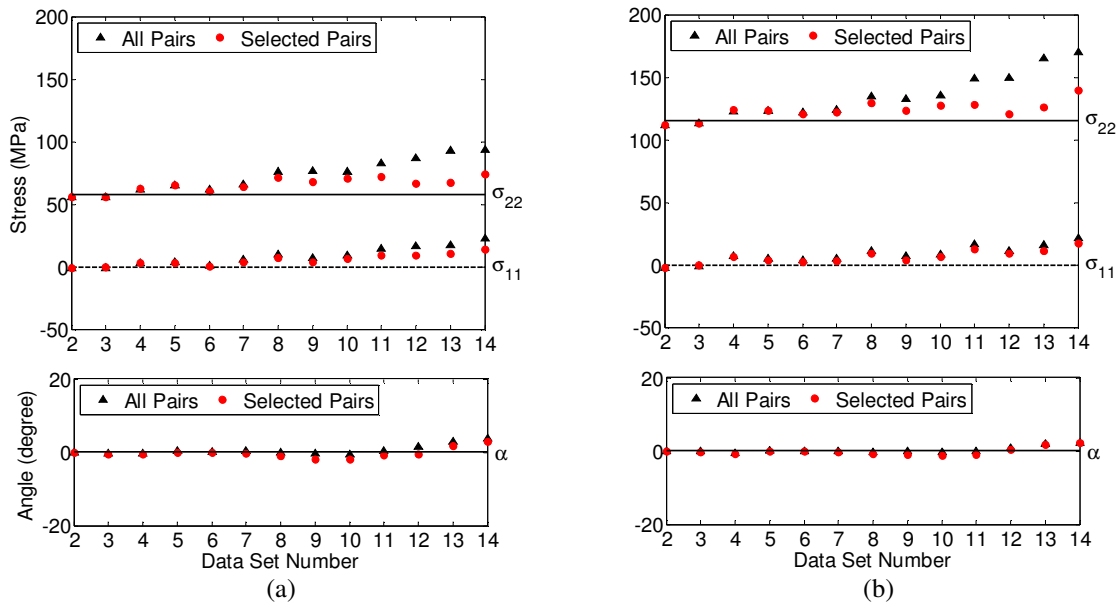


**FIGURE 9.** Estimated stresses and orientation angles for all data sets. (a)  $\sigma_{11} = 0$  MPa,  $\sigma_{22} = 57.5$  MPa,  $\alpha = 0$  degrees. (b)  $\sigma_{11} = 0$  MPa,  $\sigma_{22} = 115$  MPa,  $\alpha = 0$  degrees.

## CONCLUSIONS

This paper shows a load estimation strategy based on the assumption that the Lamb wave acoustoelastic response from a biaxial loading case can be decomposed into that from the two orthogonal uniaxial loading cases. This assumption is verified numerically, and it is further shown that only two acoustoelastic constants are needed to describe the general angle and stress dependence of a specific Lamb wave mode and frequency to a homogeneous biaxial load. Unknown applied stresses and direction can be estimated using the two acoustoelastic constants by finding the best sinusoidal fit of phase velocity changes versus propagation direction. The efficacy of the proposed strategy is verified by a fatigue test having multiple ultrasonic measurements from various uniaxial static loading conditions. A reduced set of transducer pairs was selected to improve the accuracy of the estimation results by minimizing the interference of the direct ultrasonic waves with fatigue cracks as they open under applied loads.

## ACKNOWLEDGEMENTS

This work is sponsored by the Air Force Research Laboratory under Contract No. FA8650-09-C-5206 (Charles Buynak, Program Manager).

## REFERENCES

1. N. Gandhi, J. E. Michaels and S. J. Lee, "Acoustoelastic Lamb wave propagation in a homogeneous, isotropic aluminum plate," in *Review of Progress in QNDE*, **30A**, edited by D. O. Thompson and D. E. Chimenti, AIP, pp. 161-168, 2011.
2. S. J. Lee, N. Gandhi, J. E. Michaels and T. E. Michaels, "Comparison of the effects of applied loads and temperature variations on guided wave propagation," in *Review of Progress in QNDE*, **30A**, edited by D. O. Thompson and D. E. Chimenti, AIP, pp. 175-182, 2011.
3. Y.-H. Pao and U. Gamer, "Acoustoelastic waves in orthotropic media," *J. Acoust. Soc. Am.*, **77**, pp. 806-812, 1985.
4. S. J. Lee, J. E. Michaels, X. Chen, and T. E. Michaels, "Fatigue crack detection via load-differential guided wave methods," in *Review of Progress in QNDE*, **31**, edited by D. O. Thompson and D. E. Chimenti (Eds.), AIP, expected 2012.
5. J. E. Michaels, S. J. Lee, J. S. Hall and T. E. Michaels, "Multi-mode and multi-frequency guided wave imaging via chirp excitations," in *Proc. SPIE*, **7984**, edited by T. Kundu, 79840I (11 pp), 2011.